

# LISA: A Layer-wise Integration and Suppression Approach for Hallucination Mitigation in Multimodal Large Language Models

Zhihui Guo, Xin Man, Hui Xu, Jie Shao

Shenzhen Institute for Advanced Study, University of Electronic Science and Technology of China  
 {manxin,zhihuiguo}@std.uestc.edu.cn, {huixu.kim,shaojie}@uestc.edu.cn

## Abstract

Multimodal Large Language Models (MLLMs) excel in vision-language tasks such as image captioning but remain prone to object hallucinations, where they describe objects that do not appear in the image. To mitigate this, we propose **LISA**, a **Layer-wise Integration and Suppression Approach** that enhances generation consistency through hierarchical modulation and multi-layer fusion. LISA leverages the functional hierarchy within MLLMs, where shallow layers provide visual grounding, middle layers encode semantics, and deep layers tend to amplify spurious signals. First, zone-specific spectral modulation stabilizes attention by suppressing over-amplified activations in deeper layers while preserving alignment cues in earlier layers. Second, token-level logits from selected layers are fused via anchor-based routing, with token-wise anchor selection and soft logit fusion enabling adaptive integration during decoding. LISA is fully **plug-and-play** and can be seamlessly integrated into existing MLLMs, including Qwen2.5-VL. Experiments on multiple benchmarks show that LISA reduces hallucinations by up to 53.6% in CHAIR<sub>I</sub> and improves POPE F1 by 4.5%, demonstrating strong generalization across models and tasks.

## Introduction

The rapid progress of Large Language Models (LLMs) (Floridi and Chiriatti 2020; Touvron et al. 2023; OpenAI 2023; Ru et al. 2025) has fostered Multimodal Large Language Models (MLLMs) (Liu et al. 2024b; Dai et al. 2023; Bai et al. 2023), which unify vision-language tasks such as image captioning and visual question answering. Despite these advancements, a persistent issue remains: MLLMs frequently exhibit **object hallucination** (Rohrbach et al. 2018), a specific type of hallucination where the model describes concrete objects that are not present in the image. As illustrated in Figure 1, the model incorrectly mentions a “dining” and a “table” that do not appear in the visual input, revealing a typical failure of visual grounding.

To tackle this challenge, existing studies have explored a range of solutions, including training-based (Yang et al. 2025; Liu et al. 2024a) and decoding-based (Wu et al. 2025;

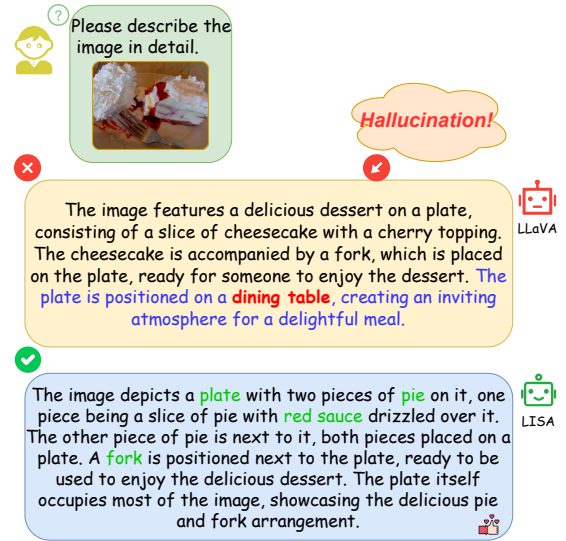


Figure 1: **An illustration of object hallucination in multimodal generation.** The upper response, generated by the LLaVA model (Liu et al. 2024b) using greedy decoding, hallucinates non-existent objects—“dining” and “table” (highlighted in red)—which are absent from the image. This reveals a typical failure of visual grounding. In contrast, the lower response, produced by LISA, provides a faithful and grounded description, free from **object hallucination**.

Yin et al. 2024; Chuang et al. 2024; Tang et al. 2025; Leng et al. 2024; Huang et al. 2024; Wang et al. 2025) approaches. Training-based methods typically optimize model parameters using hallucination-sensitive supervision. OPA-DPO (Yang et al. 2025), for instance, distills visual preference signals from the closed-source GPT-4V to guide model responses toward human-aligned outputs, but this reliance on proprietary systems limits reproducibility and transparency. In contrast, LRV-Instruction (Liu et al. 2024a) curates a large-scale instruction dataset comprising both grounded and hallucination-inducing prompts to enhance robustness via instruction tuning. Despite avoiding manual annotation, these approaches require substantial effort for dataset con-

struction and model adaptation, constraining their scalability.

Given the high cost and limited scalability of training-based methods, decoding-time strategies have emerged as scalable, training-free alternatives for hallucination mitigation. Some methods leverage external tools to enhance reasoning or verification. Bottom-Up Holistic Reasoning (Wu et al. 2025) uses external tools such as scene graph parsers, object detectors, and web search to perform structured reasoning during decoding, while Woodpecker (Yin et al. 2024) performs post-hoc multi-stage analysis to detect and correct hallucinated outputs. Other approaches focus on internal model behavior. DoLa (Chuang et al. 2024) contrasts token confidence across layers to suppress unsupported outputs; TAME (Tang et al. 2025) regularizes the query-key eigenspectrum to stabilize signal propagation; VCD (Leng et al. 2024) applies contrastive constraints on matched and mismatched visual regions; OPERA (Huang et al. 2024) re-decodes with penalties to discourage ungrounded content; and DeCo (Wang et al. 2025) fuses intermediate-layer logits to guide more grounded generation. However, most existing decoding methods treat all transformer layers as equally informative (Huang et al. 2025; Cho et al. 2025; Ru et al. 2024; Fu et al. 2025; Chen et al. 2025), without considering their functional differences. Based on empirical analysis of model behaviors across depth, we observe that MLLMs exhibit internal stratification: shallow layers contribute to visual grounding, middle layers encode semantic context, and deep layers tend to amplify unstable signals. These observations underscore the need for decoding strategies that explicitly account for functional stratification and modulate information across layer zones accordingly.

Building on this observation, we propose **LISA** (*a Layer-wise Integration and Suppression Approach*), a training-free decoding strategy designed to mitigate object hallucination. LISA explicitly leverages the hierarchical structure of multimodal transformers by partitioning the model into three functional zones—shallow, middle, and deep—to capture distinct layer-wise roles in grounding, semantic integration, and suppression. It stabilizes the attention weights via *layer-specific spectral scaling*, suppressing over-amplified, unstable signals in deeper layers while preserving stable alignment cues in shallower ones. Token-level logits from representative layers are then aggregated through cross-layer fusion and token-wise anchor routing, ensuring more reliable and faithful generation.

LISA is fully **plug-and-play**, requiring no retraining or architectural modification, and can be seamlessly applied to a variety of MLLMs. We evaluate LISA on several hallucination benchmarks, including CHAIR (Rohrbach et al. 2018), POPE (Li et al. 2023), AMBER (Wang et al. 2023), and MME (Fu et al. 2023), demonstrating consistent hallucination reduction and improved factual consistency. Our method offers a lightweight yet effective approach to enhance the reliability of multimodal generation.

Our contributions are summarized as follows:

- We identify a key limitation of existing decoding-time approaches: they overlook the functional stratification of transformer layers, leading to suboptimal integration of

layer-wise representations and insufficient modulation of spectral instability during decoding.

- We propose LISA, a training-free decoding framework that leverages the functional stratification of MLLMs. By applying layer-wise spectral modulation to stabilize attention dynamics and fusing logits across selected anchor layers, LISA effectively mitigates hallucinations.
- We conduct comprehensive evaluations on four hallucination benchmarks across multiple MLLMs. LISA consistently reduces hallucinations while preserving generation quality and demonstrates strong compatibility with diverse architectures and decoding strategies.

## Related Work

### Hallucination in MLLMs

Multimodal Large Language Models (MLLMs) unify visual and linguistic understanding to handle tasks such as image captioning and visual question answering. Despite advances in instruction tuning and cross-modal alignment (Liu et al. 2024b; Dai et al. 2023; Bai et al. 2023; Zhuang et al. 2025a; Zhang et al. 2025a; Yin et al. 2025; Zhuang et al. 2025b), MLLMs still frequently hallucinate object-level details that are unsupported by the input image, especially in complex or ambiguous scenes. These failures expose fundamental limitations in visual grounding and continue to drive research on hallucination mitigation.

### Hallucination Mitigation for MLLMs

Decoding-time strategies have received increasing attention for their training-free and plug-and-play characteristics. Methods such as DoLa (Chuang et al. 2024), DeCo (Wang et al. 2025), OPERA (Huang et al. 2024), and VCD (Leng et al. 2024) intervene during generation by reweighting logits, anchoring shallow-layer signals, or reranking outputs. While effective, these approaches often ignore the functional stratification of transformer layers, treating them as uniformly informative.

In contrast, our method LISA introduces a stratified perspective on the transformer architecture. Instead of treating all layers equivalently, LISA explicitly partitions the model into shallow, middle, and deep zones based on their observed roles in grounding visual entities, maintaining contextual coherence, and refining linguistic details. To stabilize generation, LISA performs targeted spectral modulation across these zones, dynamically suppressing unstable signals while preserving grounded information. This layered intervention enables more precise control over the generation process and improves alignment between textual outputs and visual evidence.

### Layer-wise Structure in MLLMs

Zhang et al. (2025b) conducted attention ablation analyses, revealing a staged organization within MLLMs: shallow layers propagate general visual features, intermediate layers refine object-specific details, and later layers consolidate task-specific semantics. While their investigation offers valuable interpretability, it remains primarily descriptive, abstaining

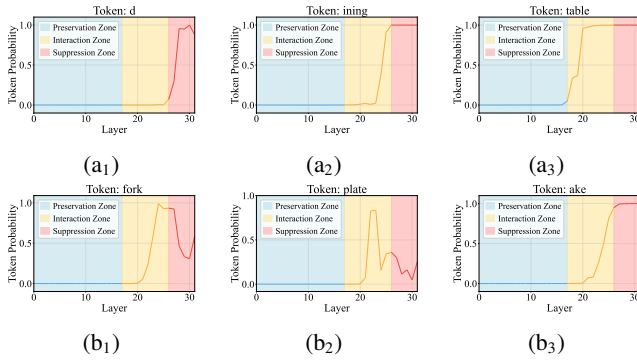


Figure 2: **Layer-wise token probabilities.** Subfigures (a<sub>1</sub>)–(a<sub>3</sub>) show hallucinated tokens; subfigures (b<sub>1</sub>)–(b<sub>3</sub>) show non-hallucinated tokens. Y-axis: token probability; X-axis: layer index (0–31).

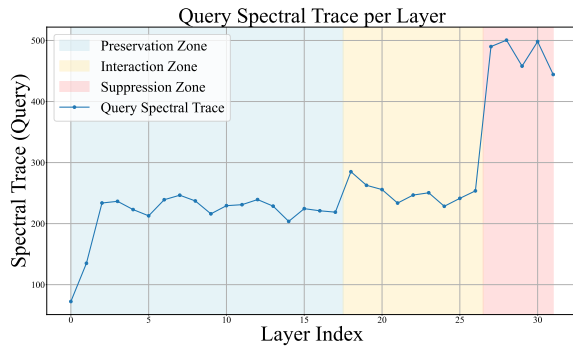


Figure 3: **Layer-wise spectral trace during token prediction.** Query spectral energy varies across layers, forming three zones: *Preservation* (blue) retains input signals; *Interaction* (yellow) builds semantic fusion; *Suppression* (red) shows spikes linked to hallucination. This pattern motivates depth-aware decoding strategies.

from a systematic exploration of how to leverage this hierarchical structure to enhance generative capabilities.

In contrast, our proposed LISA builds on this insight by explicitly treating the transformer as a functionally stratified system—dividing it into shallow, middle, and deep zones—and actively stabilizing cross-layer representations through layer-specific spectral suppression and cross-layer fusion. This design transforms descriptive observations into an effective, plug-and-play decoding mechanism that improves generation robustness without requiring retraining or architectural changes.

## Methodology

### Why Layer Matters: A Hierarchical Perspective

MLLMs produce textual responses by progressively transforming internal representations through a stack of transformer layers. While prior work (Zhang et al. 2025b) has primarily examined where modality fusion occurs, we shift focus to how grounded and hallucinated contents propagate through different depths during decoding.

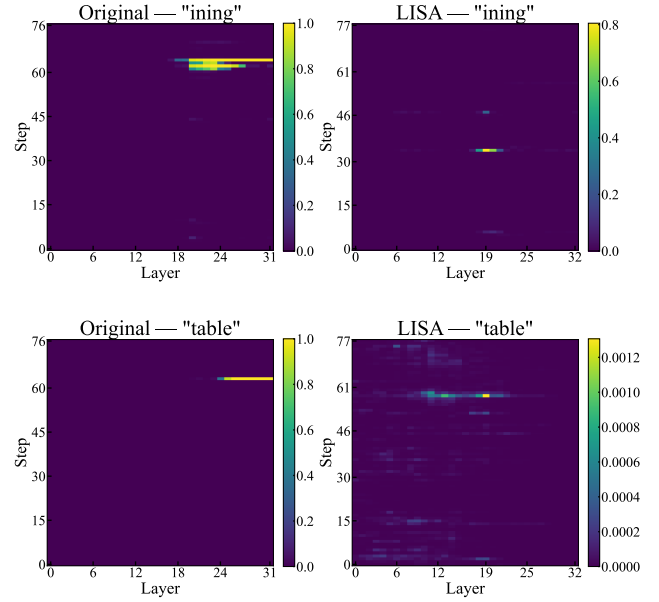


Figure 4: **Layer-wise heatmaps of hallucinated tokens.** *Left:* Greedy decoding shows sharp final-layer spikes (e.g., “ining”, “table”). *Right:* LISA suppresses unstable activations and distributes confidence across layers.

Figure 2 illustrates representative layer-wise token probabilities for hallucinated and non-hallucinated examples. Consistent with prior findings (Wang et al. 2025), hallucinated tokens often maintain persistently high probabilities in deeper layers, amplifying spurious signals. Interestingly, valid words that are split into multiple sub-tokens (e.g., cake → “c”, “ake”) can also show similar high-probability plateaus, even when they are correctly grounded. This phenomenon suggests that persistent activations in deeper layers do not always imply hallucinations, underscoring the importance of a robust, layer-wise mechanism that can dampen unstable signals without over-suppressing legitimate content.

To interpret this behavior further, Figure 3 shows the corresponding query spectral energy curves. The spectral traces mirror the probability trends: shallow layers keep energy low and dispersed, middle layers steadily integrate semantic signals, and deep layers often show abrupt spikes aligned with persistent high probabilities. Such spikes typically indicate uncontrolled activations driving hallucinations, yet they may also reflect harmless token splits. This highlights why LISA adopts a stratified spectral modulation strategy: rather than rigidly distinguishing each case, it adaptively controls layer-wise signals to mitigate hallucinations while preserving valid structures.

Figure 4 demonstrates the practical impact of our spectral modulation. Compared with existing MLLMs (Liu et al. 2024b; Dai et al. 2023; Bai et al. 2023, 2025), LISA effectively suppresses final-layer overactivation for hallucinated tokens and promotes a more balanced layer-wise activation pattern, resulting in more reliable and faithful outputs.

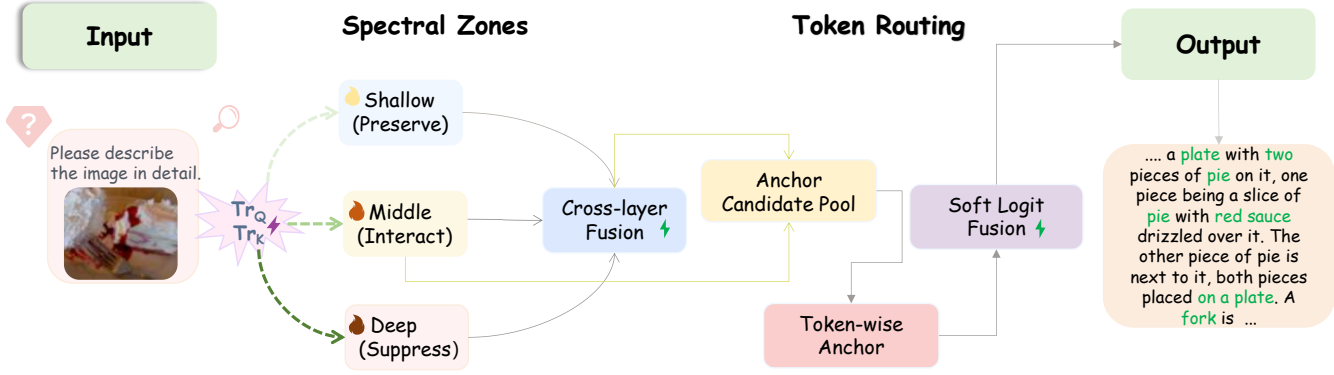


Figure 5: **Overview of LISA.** LISA stabilizes multimodal generation by modulating the layer-wise spectral energy of transformer attention. It partitions layers into three spectral zones—preservation, interaction, and suppression—reflecting the energy progression observed in query and key traces. Layer-wise spectral suppression dynamically scales attention to dampen unstable deep-layer spikes while preserving shallow and middle-layer semantics. Cross-layer token fusion aggregates stable representations across selected anchor layers, weighted by spectral stability. Finally, token-wise anchor selection and soft logit fusion adaptively integrate multi-layer signals during decoding, ensuring each token draws from the most stable layers. Together, LISA combines spectral modulation, anchor-based fusion, and token-wise routing to mitigate hallucinations while retaining depth-specific information.

Together, these observations suggest a functional hierarchy: shallow layers preserve inputs; middle layers integrate grounded semantics; deep layers tend to amplify spurious signals. Motivated by this hierarchical view, we propose LISA, which explicitly partitions the transformer into three spectral zones—preservation, interaction, and suppression, as shown in Figure 5. By combining layer-specific spectral modulation, cross-layer fusion, and token-wise anchor routing, LISA adaptively balances final-layer representation capacity with stability, mitigating hallucinations without re-training or changing parameters of MLLMs.

### Spectral Modulation for Layer-wise Stability

Motivated by prior insights (Tang et al. 2025) that controlling the query-key eigenspectrum can stabilize generation, we propose a spectral modulation mechanism that combines layer-wise spectral suppression and cross-layer token fusion to mitigate hallucinations in multimodal generation.

**Layer-wise Spectral Suppression.** For each transformer layer  $l$ , we define its spectral energy as the squared Frobenius norm of its query and key matrices:

$$\begin{aligned} \text{Tr}_Q^{(l)} &= \|\mathbf{Q}^{(l)}\|_F^2 = \text{Tr}(\mathbf{Q}^{(l)}\mathbf{Q}^{(l)\top}), \\ \text{Tr}_K^{(l)} &= \|\mathbf{K}^{(l)}\|_F^2 = \text{Tr}(\mathbf{K}^{(l)}\mathbf{K}^{(l)\top}). \end{aligned} \quad (1)$$

As shown in Figure 3, spectral energy remains low in shallow layers (preservation zone), gradually increases in middle layers (interaction zone), and often spikes in deep layers (suppression zone), aligning with the emergence of hallucinations.

To suppress unstable activations, we apply a spectral scal-

ing factor to the scaled dot-product attention:

$$\begin{aligned} \lambda_Q^{(l)} &= 1 + \frac{\gamma}{\log(\text{Tr}_Q^{(l)} + \epsilon)}, \\ \lambda_K^{(l)} &= 1 + \frac{\gamma}{\log(\text{Tr}_K^{(l)} + \epsilon)}, \end{aligned} \quad (2)$$

where  $\gamma$  controls suppression strength, and  $\epsilon$  is a small positive constant ensuring numerical stability in the logarithmic term. The modulated attention then becomes:

$$\mathbf{A}_{ij}^{(l)} = \frac{\lambda_Q^{(l)} \mathbf{Q}_i^\top \mathbf{K}_j \lambda_K^{(l)}}{\sqrt{d_k}}, \quad (3)$$

where  $d_k$  is the dimensionality of the query/key vectors, and  $\sqrt{d_k}$  serves as a normalization factor. This constrains deep-layer spikes while preserving stable shallow-layer signals.

**Cross-layer Token Fusion.** Beyond local suppression, LISA globally aggregates stable information by fusing token states across a selected anchor layer set  $\mathcal{A}$ . Rather than using all layers,  $\mathcal{A}$  consists of representative layers sampled from the three functional zones. The contribution of each layer is guided by its spectral stability:

$$s^{(l)} = \frac{1}{\text{Tr}_Q^{(l)} + \text{Tr}_K^{(l)} + \epsilon}. \quad (4)$$

Layers with lower energy have higher stability and thus contribute more. The fusion weights are normalized:

$$\alpha^{(l)} = \frac{s^{(l)}}{\sum_{j \in \mathcal{A}} s^{(j)}}, \quad \sum_{l \in \mathcal{A}} \alpha^{(l)} = 1. \quad (5)$$

The final fused representation is formulated as follows:

$$\mathbf{H}_{\text{LISA}} = \sum_{l \in \mathcal{A}} \alpha^{(l)} \mathbf{H}^{(l)}. \quad (6)$$

This amplifies grounded signals from stable layers while dampening unstable ones.

## Layer-wise Token Integration for Stable Generation

Building on stable multi-layer signals, LISA extends this stratified design into the decoding stage through token-wise anchor routing. Unlike conventional pipelines that rely solely on final-layer logits, LISA aligns the generation of each token with the layer-wise spectral pattern: grounded content stabilizes in shallow and intermediate layers, while hallucinations often correlate with unstable deep-layer spikes.

**Token-wise Anchor Selection.** To leverage this, the transformer is partitioned into three functional zones: preservation, interaction, and suppression, and representative layers from each zone are chosen as candidate anchors. The cross-layer fused representation  $\mathbf{H}_{\text{LISA}}$  is also included as a virtual anchor, expanding the anchor set to:

$$\mathcal{A} = \{\text{Interact layers}\} \cup \{\mathbf{H}_{\text{LISA}}\}. \quad (7)$$

For each token  $c$ , the anchor is dynamically selected by maximizing spectral stability:

$$l^*(c) = \arg \max_{l \in \mathcal{A}} \left( s^{(l)} \cdot \max \text{prob}_{l,c} \right), \quad (8)$$

where  $s^{(l)}$  is the spectral stability of layer  $l$ , and  $\max \text{prob}_{l,c}$  is the maximum probability of token  $c$  in layer  $l$ . This selection process ensures that the most stable layer with the highest token probability is chosen as the anchor, guiding the generation process towards more reliable and relevant content.

**Soft Logit Fusion.** Finally, token logits are fused to balance representation capacity and stability:

$$\hat{\mathbf{z}}_t(c) = (1 - \beta) \mathbf{z}_{L,t} + \beta \mathbf{z}_{l^*(c),t}, \quad \beta \in [0, 1]. \quad (9)$$

Here,  $\beta$  controls the trade-off between the capacity of the final layer and the stability of the selected anchor. Unlike the cross-layer fusion weights  $\alpha^{(l)}$  computed across layers,  $\beta$  is applied at the token level. This design allows each token to adaptively draw from either the most stable anchor or the fused representation, thereby mitigating hallucinations across decoding strategies while preserving depth-specific information.

LISA integrates multi-layer signals, enhancing the stability of token generation. By dynamically selecting the most stable anchor layer based on both spectral stability and token probability, and soft-fusing the logits, LISA minimizes hallucinations and ensures the generation of meaningful, coherent content. Together, these mechanisms yield a robust decoding approach that enhances both accuracy and stability, while preserving depth-specific information throughout the generation process.

## Experiments

### Experimental Settings

**Datasets.** We use MSCOCO (Lin et al. 2014), which contains diverse everyday scenes with human-annotated captions. Only images are used for inference; captions are for evaluation.

Hyperparameter	Value	Description
Beam size	5	Beam size
Temperature	0.7	Sampling temperature
Max tokens	512	Maximum generation length
$\beta$	0.6	Token-wise fusion weight
$\epsilon$	$10^{-7}$	Spectral stabilizer

Table 1: Main hyperparameters used in LISA.

**Baselines.** We compare LISA with standard decoding strategies (e.g., greedy decoding, beam search, and nucleus sampling) and recent decoding-time hallucination mitigation methods, including DoLa (Chuang et al. 2024), DeCo (Wang et al. 2025), VCD (Leng et al. 2024), and OPERA (Huang et al. 2024).

**Backbone Models.** We evaluate our method with four MLLMs: LLaVA (Liu et al. 2024b), InstructBLIP (Dai et al. 2023), Qwen-VL (Bai et al. 2023), and Qwen2.5-VL (Bai et al. 2025), all used in frozen form without fine-tuning.

**Implementation Details.** Main hyperparameters of LISA are given in Table 1. Due to page limit more implementation details can be found in our code repository available at <https://github.com/HanKexh/LISA>.

### Evaluation Benchmarks

**CHAIR.** The Caption Hallucination Assessment with Image Relevance (CHAIR) (Rohrbach et al. 2018) evaluates object hallucination in captions by comparing generated object mentions with ground-truth labels. It is defined as:

$$\text{CHAIR}_I = \frac{|\text{Hallucinated Objects}|}{|\text{Mentioned Objects}|},$$

$$\text{CHAIR}_S = \frac{|\text{Captions with Hallucinations}|}{|\text{All Captions}|}.$$

Following Huang et al. (2024), we evaluate on 500 MSCOCO 2014 validation images using the caption prompt: “Please describe the image in detail.”

**AMBER.** AMBER (Wang et al. 2023) evaluates hallucinations in image captions by assessing hallucinated object rate (CHAIR), coverage of ground-truth objects (Cover), proportion of hallucinated responses (Hal.), and tendency to mention cognitively biased objects (Cog.). Lower CHAIR, Hal., and Cog. indicate fewer hallucinations, while higher Cover reflects stronger grounding.

**MME.** The MME benchmark (Fu et al. 2023) evaluates the general capabilities of multimodal large language models across 14 subskills, including OCR, object recognition, spatial relations, and commonsense reasoning. It uses multiple-choice questions on natural images. We follow the official protocol and report overall accuracy.

**POPE.** The Polling-based Object Probing Evaluation (POPE) (Li et al. 2023) assesses hallucination through a binary question-answering format. For each image, the model answers whether a queried object exists in the scene. Performance is measured using the standard F1 score.

To evaluate robustness, POPE splits queried objects into three subsets: random (arbitrary samples), popular (frequent objects), and adversarial (visually similar to ground-truth).

Decoding	Method	LLaVA-1.5		InstructBLIP		Qwen-VL	
		CHAIR <sub>s</sub> ↓	CHAIR <sub>i</sub> ↓	CHAIR <sub>s</sub> ↓	CHAIR <sub>i</sub> ↓	CHAIR <sub>s</sub> ↓	CHAIR <sub>i</sub> ↓
Greedy	Vanilla	45.0	14.7	58.8	23.7	46.0	12.5
	DoLa	47.8	13.8	48.4	15.9	46.8	12.9
	DeCo	37.8	11.1	41.2	14.4	42.2	10.7
	<b>LISA</b>	<b>34.2</b> ↓10.8	<b>10.4</b> ↓4.3	<b>31.6</b> ↓27.2	<b>10.9</b> ↓12.8	<b>29.0</b> ↓17.0	<b>9.2</b> ↓3.3
Beam	Vanilla	48.8	13.9	55.6	15.8	41.8	10.8
	OPERA	44.6	12.8	46.4	14.2	34.6	9.5
	DeCo	33.0	9.7	43.8	12.7	32.0	8.7
	<b>LISA</b>	<b>29.2</b> ↓19.6	<b>9.1</b> ↓4.8	<b>31.0</b> ↓24.6	<b>11.6</b> ↓1.1	<b>20.4</b> ↓21.4	<b>7.4</b> ↓3.4
Nucleus	Vanilla	48.8	14.2	54.6	24.8	49.2	13.1
	VCD	54.0	16.0	58.0	17.0	46.4	11.9
	DeCo	42.8	13.2	43.6	<b>12.9</b> ↓11.9	43.8	11.8
	<b>LISA</b>	<b>39.0</b> ↓9.8	<b>11.6</b> ↓2.6	<b>39.4</b> ↓15.2	16.3	<b>30.2</b> ↓19.0	<b>10.3</b> ↓2.8

Table 2: **CHAIR hallucination evaluation results** for **LLaVA-1.5**, **InstructBLIP**, and **Qwen-VL** across different decoding strategies. Lower scores on CHAIR<sub>s</sub> and CHAIR<sub>i</sub> indicate fewer hallucinations. OPERA is a beam-search-based method; VCD is designed for nucleus sampling; DeCo is a general decoding-compatible approach. LISA denotes our method, and is applied consistently across all settings.

Decoding	Method	CHAIR↓	Cover↑	Hal.↓	Cog.↓
Greedy	Vanilla	8.2	48.9	34.3	4.0
	DoLa	8.0	50.8	37.5	4.3
	DeCo	6.6	47.5	28.1	2.8
	<b>LISA</b>	<b>6.5</b> ↓1.7	<b>47.2</b> ↓1.7	<b>23.1</b> ↓11.2	<b>1.9</b> ↓2.1
Beam	Vanilla	7.1	50.7	32.4	3.8
	OPERA	6.4	49.0	27.5	2.9
	DeCo	6.3	46.8	25.1	2.4
	<b>LISA</b>	<b>5.9</b> ↓1.2	<b>45.6</b> ↓5.1	<b>21.9</b> ↓10.5	<b>2.0</b> ↓1.8
Nucleus	Vanilla	10.2	50.2	43.3	4.5
	VCD	9.0	51.7	40.2	4.4
	DeCo	8.3	48.0	37.5	3.4
	<b>LISA</b>	<b>7.2</b> ↓3.0	<b>47.6</b> ↓2.6	<b>28.8</b> ↓14.5	<b>2.6</b> ↓1.9

Table 3: AMBER evaluation results of **LLaVA-1.5** under different decoding strategies. LISA consistently reduces hallucination-related metrics—**CHAIR** (hallucinated object rate), **Hal.** (rate of hallucinated responses), and **Cog.** (alignment with human cognitive biases)—while preserving **Cover**, which quantifies the proportion of ground-truth objects correctly mentioned in the response.

Each subset includes 500 MSCOCO images with six binary questions per image.

### Performance Analysis

We evaluate LISA using the four benchmarks introduced above—CHAIR, AMBER, POPE, and MME—which together capture diverse facets of generation reliability, including hallucination mitigation, visual grounding, and factual consistency across different decoding strategies and model families.

**Robust Hallucination Mitigation.** Table 2 shows that LISA consistently reduces hallucinated object mentions (CHAIR<sub>s</sub>, CHAIR<sub>i</sub>) across different models and decoding strategies on the CHAIR benchmark. These improvements are particularly evident under beam search, where LISA surpasses existing decoding-time approaches such as DoLa and DeCo, highlighting its effectiveness under conditions most prone to hallucination errors.

Similarly, as shown in Table 3, LISA significantly reduces hallucination metrics (Hal. and Cog.) while preserving grounded object coverage (Cover), demonstrating ro-

Method	LLaVA-1.5	InstructBLIP	Qwen-VL
Greedy	82.2	80.0	85.2
Nucleus	83.1	79.8	84.5
Beam	84.9	84.4	85.3
Deco	85.4	81.8	85.2
DoLa	83.2	83.4	85.8
VCD	83.1	79.9	84.7
OPERA	85.4	84.8	86.1
<b>LISA</b>	<b>86.7</b> ↑4.5	<b>84.9</b> ↑5.1	<b>86.7</b> ↑2.2

Table 4: POPE F1 scores of **LLaVA-1.5**, **InstructBLIP**, and **Qwen-VL** under various decoding strategies. Higher scores indicate stronger alignment with object existence. For fair comparison, LISA results are obtained under nucleus sampling.

bustness even in tasks requiring commonsense and spatial reasoning.

**Improved Visual Grounding and Recall.** As shown in Table 4, LISA consistently improves F1 scores on the POPE benchmark across all evaluated MLLMs, demonstrating en-



Metric	Decoding Strategy	Adversarial	Popular	Random	Avg
F1 Score	Greedy	83.50	84.30	84.00	83.93
	+LISA-flat	84.15 $\uparrow$ 0.65	84.55 $\uparrow$ 0.25	84.40 $\uparrow$ 0.40	84.37 $\uparrow$ 0.44
	+LISA	<b>84.52</b> $\uparrow$ 1.02	<b>85.41</b> $\uparrow$ 1.11	<b>85.19</b> $\uparrow$ 1.19	<b>85.04</b> $\uparrow$ 1.11
	Beam	83.42	85.84	83.33	84.20
	+LISA-flat	84.30 $\uparrow$ 0.88	86.15 $\uparrow$ 0.31	83.95 $\uparrow$ 0.62	84.80 $\uparrow$ 0.60
	+LISA	<b>86.23</b> $\uparrow$ 2.81	<b>86.87</b> $\uparrow$ 1.03	<b>88.18</b> $\uparrow$ 4.85	<b>87.09</b> $\uparrow$ 2.89
	Nucleus	83.50	84.60	84.20	84.10
	+LISA-flat	84.20 $\uparrow$ 0.70	84.95 $\uparrow$ 0.35	84.60 $\uparrow$ 0.40	84.58 $\uparrow$ 0.48
Recall	+LISA	<b>84.66</b> $\uparrow$ 1.16	<b>86.00</b> $\uparrow$ 1.40	<b>85.41</b> $\uparrow$ 1.21	<b>85.36</b> $\uparrow$ 1.26
	Greedy	68.93	68.93	68.80	68.89
	+LISA-flat	70.53 $\uparrow$ 1.60	70.67 $\uparrow$ 1.74	70.42 $\uparrow$ 1.62	70.49 $\uparrow$ 1.60
	+LISA	<b>70.73</b> $\uparrow$ 1.80	<b>70.73</b> $\uparrow$ 1.80	<b>70.55</b> $\uparrow$ 1.75	<b>70.67</b> $\uparrow$ 1.78
	Beam	68.93	77.00	67.38	71.10
	+LISA-flat	79.07 $\uparrow$ 10.14	70.53 $\downarrow$ 6.47	70.42 $\uparrow$ 3.04	73.34 $\uparrow$ 2.24
	+LISA	<b>79.60</b> $\uparrow$ 10.67	<b>79.60</b> $\uparrow$ 2.60	<b>79.68</b> $\uparrow$ 12.30	<b>79.63</b> $\uparrow$ 8.53
	Nucleus	69.00	68.93	68.87	68.93
	+LISA-flat	70.13 $\uparrow$ 1.13	70.67 $\uparrow$ 1.74	70.61 $\uparrow$ 1.74	70.47 $\uparrow$ 1.54
	+LISA	<b>71.00</b> $\uparrow$ 2.00	<b>71.13</b> $\uparrow$ 2.20	<b>70.74</b> $\uparrow$ 1.87	<b>70.96</b> $\uparrow$ 2.03

Table 5: **F1 Score and Recall on POPE of Qwen2.5-VL** across decoding strategies and subsets. **LISA-flat** applies uniform spectral modulation, while **LISA** uses adaptive, layer-specific control. LISA consistently improves over both baselines and LISA-flat.

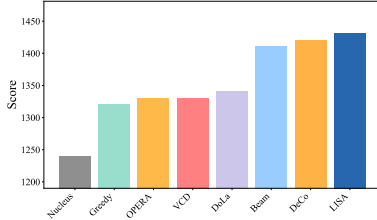


Figure 6: **MME benchmark results.** LISA outperforms standard decoding (i.e., greedy, beam, nucleus) and recent mitigation methods (i.e., DoLa, VCD, OPERA, DeCo).

hanced grounding to actual object presence. While initially developed to stabilize caption generation via stratified spectral control, LISA also enhances binary yes/no existence prediction, demonstrating its generalizability across output formats. Additional results on Qwen2.5-VL confirm that the layer-wise design of LISA reliably improves object recall and grounding under various decoding strategies.

**Consistent Improvements Across Tasks.** Finally, as shown in Figure 6, LISA achieves the highest overall score on the MME benchmark among recent decoding-time hallucination mitigation techniques, demonstrating robust performance for tasks that demand broader multimodal understanding, including spatial reasoning, attribute alignment, and fine-grained object grounding.

Across benchmarks and decoding strategies, LISA consistently enhances visual grounding and generation stability across models, offering a practical, training-free solution for mitigating hallucinations in real-world MLLM applications.

### Ablation Study

To better understand the contribution of stratified spectral control, we perform controlled comparisons using Qwen2.5-

VL as a representative testbed. Specifically, we compare the full LISA framework with a flattened variant (LISA-flat) that applies uniform spectral suppression across all layers while removing depth-specific modulation.

As shown in Table 5, both LISA and LISA-flat outperform the baseline across all decoding strategies on POPE, indicating that even uniform spectral suppression contributes to more stable signal propagation. However, LISA consistently outperforms LISA-flat, especially under beam and nucleus decodings, where hallucination risk is higher and depth-aware spectral modulation becomes increasingly important. These observations confirm that while global suppression is beneficial, explicit layer-wise adaptation is necessary to fully exploit functional differences across depths.

Overall, the results demonstrate that the stratified design of LISA is not merely an optional variant, but a critical mechanism for achieving robust and decoding-stable multimodal generation.

## Conclusion

We present LISA, a training-free decoding approach that mitigates hallucinations in MLLMs through **layer-wise integration and suppression**. Our deep analysis of token trajectories and spectral energy patterns uncovers functional distinctions across layers, motivating a stratified decoding design that preserves stable signals, facilitates semantic fusion, and suppresses unstable activations.

LISA introduces no additional training cost and is broadly applicable to existing MLLMs. Extensive experiments across multiple benchmarks validate its effectiveness in reducing hallucinations and enhancing output fidelity. These findings highlight the potential of layer-aware decoding and open new avenues for dynamic layer selection, adaptive routing, and post-hoc consistency verification.

## References

- Bai, J.; Bai, S.; Yang, S.; Wang, S.; Tan, S.; Wang, P.; Lin, J.; Zhou, C.; and Zhou, J. 2023. Qwen-VL: A Frontier Large Vision-Language Model with Versatile Abilities. *arXiv preprint arXiv:2308.12966*.
- Bai, S.; Chen, K.; Liu, X.; Wang, J.; Ge, W.; Song, S.; Dang, K.; Wang, P.; Wang, S.; Tang, J.; Zhong, H.; Zhu, Y.; Yang, M.; Li, Z.; Wan, J.; Wang, P.; Ding, W.; Fu, Z.; Xu, Y.; Ye, J.; Zhang, X.; Xie, T.; Cheng, Z.; Zhang, H.; Yang, Z.; Xu, H.; and Lin, J. 2025. Qwen2.5-VL Technical Report. *arXiv preprint arXiv:2502.13923*.
- Chen, J.; Zhang, T.; Huang, S.; Niu, Y.; Zhang, L.; Wen, L.; and Hu, X. 2025. ICT: Image-Object Cross-Level Trusted Intervention for Mitigating Object Hallucination in Large Vision-Language Models. In *IEEE/CVF Conference on Computer Vision and Pattern Recognition, CVPR 2025*, 4209–4221.
- Cho, Y.; Kim, K.; Hwang, T.; and Cho, S. 2025. Do You Keep an Eye on What I Ask? Mitigating Multimodal Hallucination via Attention-Guided Ensemble Decoding. In *The Thirteenth International Conference on Learning Representations, ICLR 2025*.
- Chuang, Y.; Xie, Y.; Luo, H.; Kim, Y.; Glass, J. R.; and He, P. 2024. DoLa: Decoding by Contrasting Layers Improves Factuality in Large Language Models. In *The Twelfth International Conference on Learning Representations, ICLR 2024*.
- Dai, W.; Li, J.; Li, D.; Tiong, A. M. H.; Zhao, J.; Wang, W.; Li, B.; Fung, P.; and Hoi, S. C. H. 2023. InstructBLIP: Towards General-purpose Vision-Language Models with Instruction Tuning. In *Advances in Neural Information Processing Systems 36: Annual Conference on Neural Information Processing Systems 2023, NeurIPS 2023*.
- Floridi, L.; and Chiriatti, M. 2020. GPT-3: Its Nature, Scope, Limits, and Consequences. *Minds Mach.*, 30(4): 681–694.
- Fu, C.; Chen, P.; Shen, Y.; Qin, Y.; Zhang, M.; Lin, X.; Yang, J.; Zheng, X.; Li, K.; Sun, X.; Wu, Y.; and Ji, R. 2023. MME: A Comprehensive Evaluation Benchmark for Multimodal Large Language Models. *arXiv preprint arXiv:2306.13394*.
- Fu, J.; Huangfu, S.; Fei, H.; Shen, X.; Hooi, B.; Qiu, X.; and Ng, S. 2025. CHiP: Cross-modal Hierarchical Direct Preference Optimization for Multimodal LLMs. In *The Thirteenth International Conference on Learning Representations, ICLR 2025*.
- Huang, Q.; Dong, X.; Zhang, P.; Wang, B.; He, C.; Wang, J.; Lin, D.; Zhang, W.; and Yu, N. 2024. OPERA: Alleviating Hallucination in Multi-Modal Large Language Models via Over-Trust Penalty and Retrospection-Allocation. In *IEEE/CVF Conference on Computer Vision and Pattern Recognition, CVPR 2024*, 13418–13427.
- Huang, W.; Zhai, Z.; Shen, Y.; Cao, S.; Zhao, F.; Xu, X.; Ye, Z.; and Lin, S. 2025. Dynamic-LLaVA: Efficient Multimodal Large Language Models via Dynamic Vision-language Context Sparsification. In *The Thirteenth International Conference on Learning Representations, ICLR 2025*.
- Leng, S.; Zhang, H.; Chen, G.; Li, X.; Lu, S.; Miao, C.; and Bing, L. 2024. Mitigating Object Hallucinations in Large Vision-Language Models through Visual Contrastive Decoding. In *IEEE/CVF Conference on Computer Vision and Pattern Recognition, CVPR 2024*, 13872–13882.
- Li, Y.; Du, Y.; Zhou, K.; Wang, J.; Zhao, W. X.; and Wen, J. 2023. Evaluating Object Hallucination in Large Vision-Language Models. In *Proceedings of the 2023 Conference on Empirical Methods in Natural Language Processing, EMNLP 2023*, 292–305.
- Lin, T.; Maire, M.; Belongie, S. J.; Hays, J.; Perona, P.; Ramanan, D.; Dollár, P.; and Zitnick, C. L. 2014. Microsoft COCO: Common Objects in Context. In *Computer Vision - ECCV 2014 - 13th European Conference, Zurich, Switzerland, September 6-12, 2014, Proceedings, Part V*, 740–755.
- Liu, F.; Lin, K.; Li, L.; Wang, J.; Yacoob, Y.; and Wang, L. 2024a. Mitigating Hallucination in Large Multi-Modal Models via Robust Instruction Tuning. In *The Twelfth International Conference on Learning Representations, ICLR 2024*.
- Liu, H.; Li, C.; Li, Y.; and Lee, Y. J. 2024b. Improved Baselines with Visual Instruction Tuning. In *IEEE/CVF Conference on Computer Vision and Pattern Recognition, CVPR 2024*, 26286–26296.
- OpenAI. 2023. GPT-4 Technical Report. *arXiv preprint arXiv:2303.08774*.
- Rohrbach, A.; Hendricks, L. A.; Burns, K.; Darrell, T.; and Saenko, K. 2018. Object Hallucination in Image Captioning. In *Proceedings of the 2018 Conference on Empirical Methods in Natural Language Processing*, 4035–4045.
- Ru, J.; Tian, J.; Xiao, C.; Li, J.; and Shen, H. T. 2024. Imbalanced Open Set Domain Adaptation via Moving-Threshold Estimation and Gradual Alignment. *IEEE Trans. Multim.*, 26: 2504–2514.
- Ru, J.; Xie, Y.; Zhuang, X.; Yin, Y.; and Zou, Y. 2025. Do we really have to filter out random noise in pre-training data for language models? *arXiv preprint arXiv:2502.06604*.
- Tang, F.; Huang, Z.; Liu, C.; Sun, Q.; Yang, H.; and Lim, S. 2025. Intervening Anchor Token: Decoding Strategy in Alleviating Hallucinations for MLLMs. In *The Thirteenth International Conference on Learning Representations, ICLR 2025*.
- Touvron, H.; Lavril, T.; Izacard, G.; Martinet, X.; Lachaux, M.; Lacroix, T.; Rozière, B.; Goyal, N.; Hambro, E.; Azhar, F.; Rodriguez, A.; Joulin, A.; Grave, E.; and Lample, G. 2023. LLaMA: Open and Efficient Foundation Language Models. *arXiv preprint arXiv:2302.13971*.
- Wang, C.; Chen, X.; Zhang, N.; Tian, B.; Xu, H.; Deng, S.; and Chen, H. 2025. MLLM can see? Dynamic Correction Decoding for Hallucination Mitigation. In *The Thirteenth International Conference on Learning Representations, ICLR 2025*.
- Wang, J.; Wang, Y.; Xu, G.; Zhang, J.; Gu, Y.; Jia, H.; Wang, J.; Xu, H.; Yan, M.; Zhang, J.; and Sang, J. 2023. AMBER: An LLM-free Multi-dimensional Benchmark for MLLMs Hallucination Evaluation. *arXiv preprint arXiv:2311.07397*.



Wu, S.; Fei, H.; Pan, L.; Wang, W. Y.; Yan, S.; and Chua, T. 2025. Combating Multimodal LLM Hallucination via Bottom-Up Holistic Reasoning. In *AAAI-25, Sponsored by the Association for the Advancement of Artificial Intelligence*, 8460–8468.

Yang, Z.; Luo, X.; Han, D.; Xu, Y.; and Li, D. 2025. Mitigating Hallucinations in Large Vision-Language Models via DPO: On-Policy Data Hold the Key. In *IEEE/CVF Conference on Computer Vision and Pattern Recognition, CVPR 2025*, 10610–10620.

Yin, S.; Fu, C.; Zhao, S.; Xu, T.; Wang, H.; Sui, D.; Shen, Y.; Li, K.; Sun, X.; and Chen, E. 2024. Woodpecker: hallucination correction for multimodal large language models. *Sci. China Inf. Sci.*, 67(12).

Yin, Y.; Xie, Y.; Yang, W.; Yang, D.; Ru, J.; Zhuang, X.; Liang, L.; and Zou, Y. 2025. ATRI: Mitigating Multilingual Audio Text Retrieval Inconsistencies by Reducing Data Distribution Errors. In *Proceedings of the 63rd Annual Meeting of the Association for Computational Linguistics, ACL 2025, Vienna, Austria, July 27–August 1, 2025*.

Zhang, P.; Su, Y.; Wu, P.; An, D.; Zhang, L.; Wang, Z.; Wang, D.; Ding, Y.; Zhao, B.; and Li, X. 2025a. Cross from Left to Right Brain: Adaptive Text Dreamer for Vision-and-Language Navigation. *arXiv preprint arXiv:2505.20897*.

Zhang, Z.; Yadav, S.; Han, F.; and Shutova, E. 2025b. Cross-modal Information Flow in Multimodal Large Language Models. In *IEEE/CVF Conference on Computer Vision and Pattern Recognition, CVPR 2025, Nashville, TN, USA, June 11-15, 2025*, 19781–19791.

Zhuang, X.; Xie, Y.; Deng, Y.; Liang, L.; Ru, J.; Yin, Y.; and Zou, Y. 2025a. VARGPT: Unified Understanding and Generation in a Visual Autoregressive Multimodal Large Language Model. *arXiv preprint arXiv:2501.12327*.

Zhuang, X.; Xie, Y.; Deng, Y.; Yang, D.; Liang, L.; Ru, J.; Yin, Y.; and Zou, Y. 2025b. VARGPT-v1.1: Improve Visual Autoregressive Large Unified Model via Iterative Instruction Tuning and Reinforcement Learning. *arXiv preprint arXiv:2504.02949*.